

# Simultaneous Pressure and Optical Measurements of Nanoaluminum Thermites: Investigating the Reaction Mechanism

K. Sullivan\* and M. R. Zachariah†  
*University of Maryland, College Park, Maryland 20740*

DOI: 10.2514/1.45834

This work investigates the reaction mechanism of metastable intermolecular composites by collecting simultaneous pressure and optical signals during combustion in a constant-volume pressure cell. Nanoaluminum and three different oxidizers are studied: CuO, SnO<sub>2</sub>, and Fe<sub>2</sub>O<sub>3</sub>. In addition, these mixtures are blended with varying amounts of WO<sub>3</sub> as a means to perturb the gas release in the system. The mixtures with CuO and SnO<sub>2</sub> exhibit pressure signals that peak on timescales faster than the optical signal, whereas the mixtures containing Fe<sub>2</sub>O<sub>3</sub> do not show this behavior. The burn time is found to be relatively constant for both CuO and SnO<sub>2</sub>, even when a large amount of WO<sub>3</sub> is added. For Fe<sub>2</sub>O<sub>3</sub>, the burn time decreases as WO<sub>3</sub> is added, and the temperature increases. The results are consistent with the idea that oxidizers such as CuO and SnO<sub>2</sub> decompose and release gaseous oxidizers fast, relative to the burning, and this is experimentally seen by an initial pressure rise followed by a prolonged optical emission. In this case, the burning is rate limited by the aluminum, and it is speculated to be similar to the burning of aluminum in a pressurized oxygenated environment. For the Fe<sub>2</sub>O<sub>3</sub> system, the pressure and optical signals occur concurrently, indicating that the oxidizer decomposition is the rate-limiting step.

## I. Introduction

METASTABLE intermolecular composites (MICs) are a class of energetic materials consisting of an intimate mixture of fuel and oxide nanoparticles. Aluminum is primarily used as the fuel, and a variety of metal oxides have been used, including but not limited to CuO, WO<sub>3</sub>, MoO<sub>3</sub>, Bi<sub>2</sub>O<sub>3</sub>, and Fe<sub>2</sub>O<sub>3</sub>. MICs are a relatively new class of energetic materials, and research efforts to understand them have increased since Aumann et al. [1] reported a  $\sim 1000\times$  increase in reactivity when nano-sized Al/MoO<sub>3</sub> particles were used in place of their micron-sized counterparts. The high energy density and wide range of tunability of MICs make them attractive candidates for uses in propellants, pyrotechnics, and explosives. However, the reaction mechanism is still very poorly understood.

A commonly used technique to prepare MICs is to ultrasonicate the powders in a dispersing liquid, such as hexane or isopropyl alcohol, and then allow the liquid to dry. The remaining powder can be broken up or sieved until it has the consistency of a loose powder. A variety of experimental methods have been used to investigate the reactivity of these powders, including thermal analysis [2,3], combustion in a shock tube [4], flame propagation in open channels [5–11] and tubes [12–14], heated filament studies [3], and constant-volume pressure cells [6,15–19]. The pressure signal and/or optical emission can be collected to investigate the reactivity of these materials. The pressurization rate has been shown to correlate with flame propagation velocities [20] and is typically reported as a relative measurement of reactivity. Other authors [12,14] have shown a correlation between the peak pressure and the propagation velocity. Recently, authors [12–14] have used an instrumented burn tube to collect the optical and pressure signals simultaneously.

If the reaction is self-propagating, there are three phenomena occurring simultaneously: ignition of the material, reaction between

the fuel and oxidizer, and energy propagation. None of these phenomena themselves are well understood for nanoparticles, especially when the heating rate is high, as is the case in combusting systems. Nanoaluminum has been shown to have a much lower ignition temperature than micron-sized aluminum. Although both have a naturally formed oxide shell surrounding the elemental core, in the nanoparticle, the oxide shell can account for a relatively large portion of the particle's mass. Upon heating, the aluminum core melts at a much lower temperature than the oxide shell (933 vs 2327 K) and can expand, inducing stresses on the oxide shell. The response of the shell to this expansion may be different for a nanoparticle vs a large particle, leading to a lower ignition temperature. Some authors argue that a decomposition or phase change in the shell occurs, thus allowing aluminum to diffuse outward [21–23], whereas other authors argue that the rapid expansion of the core induces enough stress to completely shatter the shell and unload the aluminum as small liquid clusters [24–26]. The burning mechanism of aluminum thereafter will be quite different, depending on what mechanism of ignition happens.

The burning mechanism of nanoaluminum particles is currently poorly understood. For combustion-type applications, the heating rate of nanoparticles will be high ( $10^6$ – $10^8$  K/s). Experiments should be designed to reproduce these heating rates, and one such experimental technique that accomplishes this is a shock tube. Bazyn et al. [27,28] studied the combustion of nanoaluminum at elevated temperatures and pressures in a shock tube. The authors combust aluminum at varying temperatures, pressures, and oxygen mole fractions, and they use three-color pyrometry to measure the particle temperature. The authors show that the ambient temperature plays a significant roll on the aluminum combustion, indicating that heat losses are much more important for nanoparticles than for larger-sized particles. The same authors [29] show that a transition from a diffusion to a kinetic-limited mechanism begins to occur below a critical particle size,  $\sim 10$   $\mu\text{m}$ . For a kinetic-limited mechanism, the flame sits closer to (if not on) the particle surface, and the flame temperature is limited by the boiling point of aluminum.

The third phenomena occurring in the reaction mechanism of a self-propagating MIC is energy propagation, and authors [12,30] have shown that the dominant mode of energy propagation through a loose powder is convection. As a result, MICs often exhibit an optimal reactivity that correlates with gas production instead of temperature. For example, Sanders et al. [12] found that Al/CuO has

Received 4 June 2009; revision received 11 January 2010; accepted for publication 22 January 2010. Copyright © 2010 by Michael R. Zachariah. Published by the American Institute of Aeronautics and Astronautics, Inc., with permission. Copies of this paper may be made for personal or internal use, on condition that the copier pay the \$10.00 per-copy fee to the Copyright Clearance Center, Inc., 222 Rosewood Drive, Danvers, MA 01923; include the code 0748-4658/10 and \$10.00 in correspondence with the CCC.

\*Department of Mechanical Engineering.

†Department of Mechanical Engineering and Department of Chemistry and Biochemistry; mrz@umd.edu.

a peak reactivity for an equivalence ratio very near stoichiometric. The authors use equilibrium calculations to show that a stoichiometric mixture produces the maximum amount of Cu gas, and any deviation from this mixture will lower the temperature, hindering the gas production, and thus the convective mode of energy propagation. Conversely, other mixtures often exhibit enhanced reactivity for slightly fuel-rich mixtures. The same authors show that an Al/Bi<sub>2</sub>O<sub>3</sub> thermite has a greater propagation velocity and peak pressure for an equivalence ratio of 1.3 when compared with an equivalence ratio of 1.0, even though the calculated adiabatic flame temperature is a few hundred degrees lower at the fuel-rich condition. Also, Al/MoO<sub>3</sub> shows an optimal reactivity for an equivalence ratio around 1.2–1.4. The enhancement is attributed to increased gas production for the fuel-rich conditions and is predicted by thermodynamic equilibrium calculations.

Both Sanders et al. [12] and Malchi et al. [14] show that the peak pressure correlates with the flame propagation velocity. In the two works, an instrumented burn tube is used to simultaneously collect the pressure and optical signals. The authors use equilibrium calculations to show correlations between the predicted equilibrium gas and the experimental trends in pressure. From Fig. 9 in Malchi et al. [14], it appears that the optical signal reaches its peak on the same time scale as the pressure does,  $\sim 10 \mu\text{s}$ .

## II. Thermochemistry of Mixtures

Recent mass spectrometry work by our group has indicated that oxygen release from the metal oxide decomposition is important in the reaction mechanism of thermites, in particular for CuO and Fe<sub>2</sub>O<sub>3</sub>. The current work expands on this idea to investigate the burning of nanoaluminum composites in a constant-volume pressure cell. The pressure and optical signals are collected simultaneously to have two different measurements of reactivity. The oxides studied are CuO, Fe<sub>2</sub>O<sub>3</sub>, and SnO<sub>2</sub>. These particular oxidizers have adiabatic flame temperatures at or above the boiling point of the metal in the metal oxide, and the gas is predicted to be almost entirely composed of this metal at equilibrium. These oxidizers also decompose to suboxides and gaseous oxidizers, which will be discussed in more detail later. The calculated equilibrium for stoichiometric mixtures of these oxidizers with aluminum is shown in Table 1. The CHEETAH 4.0 code was used with the JCZS product library [31], as recommended by Sanders et al. [12]. The mixture density was assumed to be 0.00192 g/cc, because we always react 25 mg of material in our 13 cc cell. The experimental pressurization rate is also given for comparison.

We will start by investigating the simultaneous pressure and optical signals for the three oxidizers mentioned previously. We will then go on to perturb the system by adding increasing amounts of WO<sub>3</sub> in place of the metal oxide. We chose WO<sub>3</sub> because, when added as the minor component, the adiabatic temperature remains relatively unchanged. Also, WO<sub>3</sub> is predicted to produce very little equilibrium gas and does not decompose to O<sub>2</sub> or any significant gaseous oxidizing species until greater than 2800 K. All blends are stoichiometric and are referred to in terms of the molar percentage of WO<sub>3</sub> in the oxidizer. For example, a 40% WO<sub>3</sub> mixture means that 40% of the oxidizer molecules are WO<sub>3</sub>, 60% are the other oxidizer, and the corresponding amount of aluminum is added to make the overall mixture stoichiometric, assuming complete conversion to Al<sub>2</sub>O<sub>3</sub>.

## III. Experimental

The aluminum used in this study was purchased from the Argonide Corporation and is designated as 50 nm ALEX by the supplier. The aluminum was found to be 70% active by mass, as measured by thermogravimetric analysis. All other materials were purchased from Sigma Aldrich and have average particle diameters of less than 100 nm, as specified by the supplier. All samples were prepared by weighing out the powder and adding it to a ceramic crucible. Approximately 10 ml of hexane was added, and the mixtures were ultrasonicated in a sonicating bath for 30 min to ensure intimate mixing. The samples were then placed in a fume hood until the hexane evaporated and the wetness was gone, and then the samples were put in a 100°C furnace for a few minutes to drive off any remaining hexane. The dry powders were very gently broken up with a Teflon-coated spatula until the consistency was that of a loose powder. Appropriate equipment (antistatic mats and wrist straps, along with basic lab safety equipment, such as gloves and goggles) should be used when handling the dried powder in order to minimize the risk of accidental ignition and injury.

A fixed mass (25 mg) of the powder was weighed out and placed in a small (13 cc free volume) combustion cell. The sample sits in a bowl-shaped sample holder, and a Nichrome coil contacts the top of the powder so the reaction propagates downward and into the holder upon ignition. Two ports (located on the sides of the cell) were used to collect the pressure and optical signal simultaneously. In one port, a lens tube assembly, containing a plano-convex lens ( $f = 50 \text{ mm}$ ), collected light and imaged onto an optical fiber coupled to a high-speed Si photo detector (1 ns rise time, model DET10A, Thorlabs). In the second port, a piezoelectric pressure sensor was employed, the details for which can be found in Prakash et al. [17].

The powder is ignited by manually increasing the voltage and current until the sample is ignited. This is done as rapidly as possible to avoid significant heating of the powder. The data collection was triggered by the rising optical signal. There is always an  $\sim 60 \mu\text{s}$  delay between the onset of the optical emission and the onset of the pressure signal. This is due to the time delay between the optical triggering and when the pressure wave arrives at the sensor, a few centimeters away. The pressure data were thus shifted in time for the analysis so that the onset of the pressure and light are shown to occur simultaneously.

## IV. Results and Discussion

We first show the simultaneous pressure and optical signals for pure Al/CuO, Al/SnO<sub>2</sub>, and Al/Fe<sub>2</sub>O<sub>3</sub> in Fig. 1. Also included is pure Al/WO<sub>3</sub> for comparison. Note that the axes for each plot have all been adjusted to fill the plot area. From Fig. 1, we can immediately see that CuO and SnO<sub>2</sub> exhibit a pressure peak well before the optical signal reaches its peak. In the case of Fe<sub>2</sub>O<sub>3</sub> and WO<sub>3</sub>, the pressure and optical signals occur concurrently.

It is important to take a moment to discuss our interpretation of the optical signal and the various considerations that may complicate the analysis. First of all, an accurate measurement of the temperature for such a large sample is greatly complicated by the fact that the viewing area is optically thick, and thus the measurement would be biased to the outermost (or coolest) region of the reaction. Also, we have no reason to believe that the flame region would be spatially homogeneous. It is possible that the optical signal could be measuring the emission from large chunks of material that ignite later in time;

**Table 1** Calculated temperature and gas production for stoichiometric mixtures of various metal oxides with nanoaluminum

Metal oxide	Boiling point metal, K	Tad (Cheetah UV), K	Moles gas/kg reactant	Contribution of metal to the total gas, %	Experimental pressurization rate, psi/ $\mu\text{s}$
CuO	2837	2967	3.5	97	11.1
SnO <sub>2</sub>	2533	2573	2.2	94	7.7
Fe <sub>2</sub> O <sub>3</sub>	3023	2834	0.52	98	0.017
WO <sub>3</sub>	5933	3447	0.13	<0.01	0.028

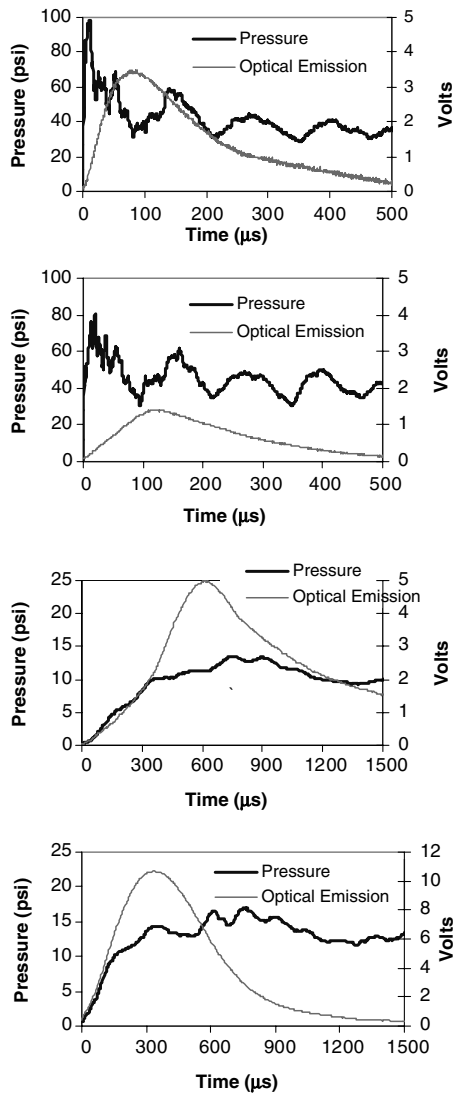


**Fig. 1** Simultaneous optical and pressure signals from top to bottom: Al/CuO, Al/SnO<sub>2</sub>, and Al/Fe<sub>2</sub>O<sub>3</sub>. Also shown is Al/WO<sub>3</sub> (bottom).

however, we do not believe this to be the case, because we do see actual evidence of this occasionally (i.e., a bump in the optical signal after the peak). The experimental data shown in Fig. 1 are for a sample mass of 25 mg. To determine whether the sample mass had any effect on the optical signal, we also repeated this for a sample mass of 10 mg. In this case, we see a decrease in the pressure signal (as expected) but no change in the optical signal. The relative intensities of the optical signal are qualitatively consistent with what would be expected, based on adiabatic flame temperature calculations (i.e., Al/WO<sub>3</sub> is the hottest/brightest and Al/SnO<sub>2</sub> is the coolest/weakest, with Al/CuO and Al/Fe<sub>2</sub>O<sub>3</sub> being in between). Optical emission generally signifies a combustion event is occurring, and the intensity is highly sensitive to the temperature of radiating particles ( $\sim T^4$ ). Therefore, we will simply use the optical measurement as a relative measurement of the system temperature, and we assume that the full-width half-maximum (FWHM) of the optical signal is capturing the burn time of the average-sized particles in the system.

Now that the optical emission has been discussed, we see from Fig. 1 that, for the Al/CuO and Al/SnO<sub>2</sub> systems, the pressurization is happening well before the system temperature is at its peak value. These systems have adiabatic flame temperatures near the boiling point of the metal (Cu and Sn), and so the vaporization of the metal should not occur until the temperature is near its hottest point. This is clearly not the case for these two systems, thus the pressure rise is likely caused by something else.

An alternate explanation is that the pressure rise is attributed to the decomposition of the oxidizer. We have recently investigated this idea for the Al/Fe<sub>2</sub>O<sub>3</sub> and Al/CuO thermite system using fast-heating wire experiments coupled with mass spectrometry. Upon rapid heating, a significant O<sub>2</sub> signal emerges first, followed by other species indicative of the reaction (i.e., Al<sub>2</sub>O<sub>3</sub>, Cu, and Fe). The O<sub>2</sub> signal is a product of the thermal decomposition of the metal oxide in the case of both CuO and Fe<sub>2</sub>O<sub>3</sub>. An enhancement in the O<sub>2</sub> release (relative to the pure oxidizer) is seen for the thermite, indicating that some energy from the reaction further decomposes the oxidizer.

To illustrate this, we perform constant temperature and pressure calculations using the NASA CEA equilibrium code to show the decomposition behaviors of the metal oxides. The equilibrium species distribution at atmospheric pressure is shown as a function of temperature in Fig. 2. The markers indicate the point at which no oxygen-containing species remain in the condensed phase [i.e., Cu<sub>2</sub>O(L) or Fe<sub>3</sub>O<sub>4</sub>(L), decomposition products of CuO and Fe<sub>2</sub>O<sub>3</sub>]. For all three oxidizers, we see the emergence of O<sub>2</sub> when the temperature reaches a certain value and the metal oxide decomposes to a suboxide and O<sub>2</sub>. In the case of SnO<sub>2</sub>, a significant amount of SnO gas is also formed during decomposition; therefore, we have lumped the O<sub>2</sub> and SnO together into one quantity, because both are gaseous decomposition products and are likely important in oxidizing the aluminum. Note that we do not include WO<sub>3</sub> in Fig. 2, because WO<sub>3</sub> does not thermally decompose into significant amounts of O<sub>2</sub>. Instead, the calculations show the emergence of other oxide species [i.e. WO<sub>2</sub>, WO<sub>3</sub>, and (WO<sub>3</sub>)<sub>x</sub>].

From Fig. 2, we see an interesting observation: CuO and SnO<sub>2</sub> fully decompose to gaseous oxidizing species at temperatures below their adiabatic flame temperatures. In contrast, Fe<sub>2</sub>O<sub>3</sub> does not fully decompose until greater than 3200 K, several hundred degrees above its adiabatic temperature. From the experimental data and the arguments previously mentioned, it is reasonable to speculate that the decomposition of CuO and SnO<sub>2</sub> is what leads to the first pressure spike, followed by a much longer optical trace as the aluminum continues to burn. In the case of Fe<sub>2</sub>O<sub>3</sub>, the oxidizer cannot efficiently decompose; therefore, the decomposition may, in fact, be the rate-limiting step. We must emphasize that we are not implying that the oxidizer has completely decomposed within the pressure rise time (we also have no way to prove that it has not). Instead, we are simply using the thermodynamic calculations to suggest that CuO and SnO<sub>2</sub> may decompose more efficiently than Fe<sub>2</sub>O<sub>3</sub> because of the nature of the adiabatic and decomposition temperatures, whereas this is not the case for Fe<sub>2</sub>O<sub>3</sub>. The extent of decomposition or the decomposition pathway under such high heating rates is not something we can currently measure within the pressure rise time. That being said, we now turn to the experimental results in which WO<sub>3</sub> is added.

The experimental pressurization rate is shown as a function of WO<sub>3</sub> for the three systems in Fig. 3. For both the CuO and SnO<sub>2</sub> systems, the optimum reactivity occurs when no WO<sub>3</sub> is added, and it drops significantly when even a small amount of WO<sub>3</sub> is introduced.

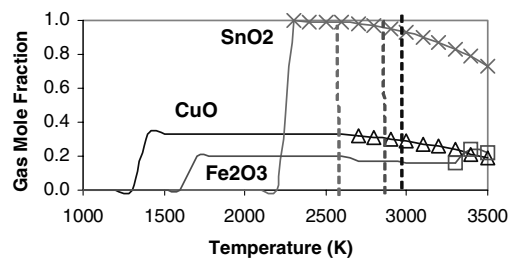


**Fig. 2** Gas release from oxidizer decomposition as a function of temperature. The gas is O<sub>2</sub> for all oxidizers and includes SnO(g) for the SnO<sub>2</sub>. The markers indicate the points at which no oxygen remains in the condensed phase. The vertical lines show the adiabatic temperature for reference, from left to right: SnO<sub>2</sub>, Fe<sub>2</sub>O<sub>3</sub>, and CuO. Constant temperature and pressure calculations, assuming  $P = 1$  atm for all runs. Note that WO<sub>3</sub> is not included, because it does not decompose to O<sub>2</sub> upon its decomposition (greater than 2800 K).

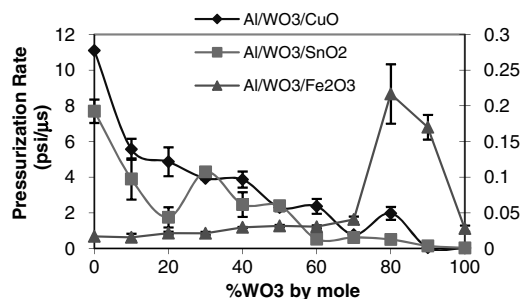


Fig. 3 Experimental pressurization rate as a function of the molar percentage of  $\text{WO}_3$  in the oxidizer. The  $\text{Al}/\text{WO}_3/\text{Fe}_2\text{O}_3$  data are plotted on the secondary axis.

For the  $\text{Fe}_2\text{O}_3$ , we see a significant enhancement and peak reactivity when the mixture is 80%  $\text{WO}_3$ . Clearly, something in the blended  $\text{Fe}_2\text{O}_3/\text{WO}_3$  system is enhancing the pressurization rate above either system alone.

To show whether the trends in the experimental pressurization rate could be explained by oxidizer decomposition, we seek some way to estimate the gaseous oxidizer ( $\text{O}_2$  and  $\text{SnO}$ ) release rate. Because knowledge of these rates is not well known, we assume the oxidizer decomposition and the gas release rate are proportional to the number of moles of the decomposing species in the mixture ( $\text{CuO}$ ,  $\text{SnO}_2$ , or  $\text{Fe}_2\text{O}_3$ ). Because  $\text{WO}_3$  does not show any decomposition products and gas release until greater than 2800 K, we are fairly certain that  $\text{WO}_3$  does not contribute to the initial pressure rise, at least in the  $\text{CuO}$  and  $\text{SnO}_2$  systems. We chose to use pressurization rate rather than peak pressure as a measure of kinetics, because a peak pressure analysis can most easily be correlated only if one can assume complete decomposition of the oxidizer. The pressurization rate and predicted oxidizer release rate are plotted for the three systems in Fig. 4. The values have been normalized by the maximum.

We see that the pressurization rate does, indeed, correlate with the predicted oxidizer release rate for the  $\text{CuO}$  and  $\text{SnO}_2$  systems but not for  $\text{Fe}_2\text{O}_3$ . This is further support that the pressurization rate is attributed to the oxidizer decomposition for the  $\text{CuO}$  and  $\text{SnO}_2$ . For the  $\text{Fe}_2\text{O}_3$  system, the predicted oxygen release does not correlate with the trend in the pressurization rate at all. We see a constant value of the pressurization rate up until about 70%  $\text{WO}_3$ , followed by a sharp jump to a peak at 80% and then a decrease from 90–100%  $\text{WO}_3$ . One explanation for this behavior could be that the formation of  $\text{Fe}$  gas causes this peak; however, this does not explain why the pressurization rate is constant over such a wide range (0–70%). As  $\text{WO}_3$  is added, we would expect the amount of  $\text{Fe}$  gas to change and affect the pressurization rate, but this was not observed. A more likely explanation is that the temperature reaches a high enough value to decompose the  $\text{Fe}_2\text{O}_3$  efficiently. As discussed previously and shown in Fig. 2, the adiabatic flame temperature of  $\text{Al}/\text{Fe}_2\text{O}_3$  is lower than the point at which  $\text{Fe}_2\text{O}_3$  can fully decompose. As  $\text{WO}_3$  is added, the adiabatic temperature increases, and it is likely that at 80 and 90%  $\text{WO}_3$ , the temperature becomes high enough to efficiently decompose the  $\text{Fe}_2\text{O}_3$ . To corroborate this idea, the raw data are shown for 70 and 80%  $\text{WO}_3$  in the  $\text{Al}/\text{WO}_3/\text{Fe}_2\text{O}_3$  system in Fig. 5. What can be seen is that, for 80%  $\text{WO}_3$ , the first pressure peak occurs well before the optical peak, whereas this is not the case for 70%. This is consistent with the idea that the system temperature reaches a point at which the  $\text{Fe}_2\text{O}_3$  can decompose efficiently, leading to a fast pressure spike relative to the burning.

We can use the results and discussion thus far to make some speculations about the reaction mechanism. For systems in which the adiabatic flame temperature is high enough and heat transfer is not limiting, when the fuel begins to burn, the oxidizer can decompose and pressurize the system faster than the reaction time scale. The fuel then continues to burn over a longer period, as can be seen in Fig. 1 for the  $\text{CuO}$  and  $\text{SnO}_2$ . Systems such as these would thus be rate limited by the mechanism by which the aluminum burns in a gaseous oxidizing environment. For an oxidizer such as  $\text{Fe}_2\text{O}_3$ , the adiabatic flame temperature is below the point at which the oxidizer can fully

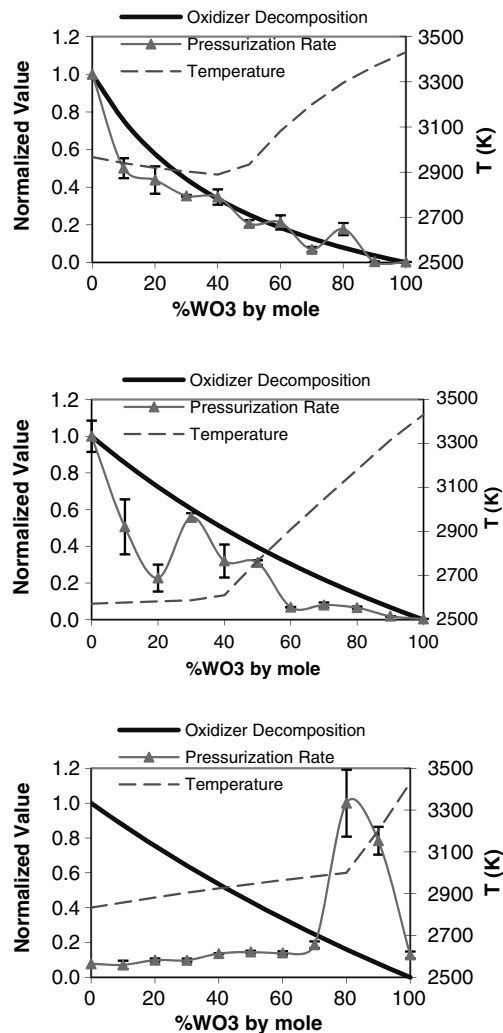


Fig. 4 Gas release prediction and experimental pressurization rate (both normalized by the maximum value), along with the adiabatic temperature. Systems from top to bottom are  $\text{Al}/\text{WO}_3/\text{CuO}$ ,  $\text{Al}/\text{WO}_3/\text{SnO}_2$ , and  $\text{Al}/\text{WO}_3/\text{Fe}_2\text{O}_3$ .

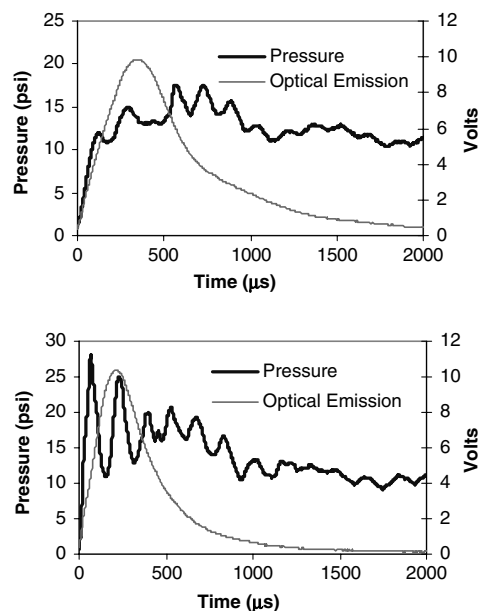


Fig. 5 Raw data for the 70% (top) and 80% (bottom)  $\text{WO}_3$  mixtures of  $\text{Al}/\text{WO}_3/\text{Fe}_2\text{O}_3$ . Note how the first major pressure peak occurs earlier than the optical peak for the 80%  $\text{WO}_3$  mixture.

decompose, thus the oxidizer cannot decompose efficiently. The burning mechanism in this case is rate limited by the oxidizer decomposition and oxygen release. The fact that the optical and pressure signals occur concurrently for  $\text{Fe}_2\text{O}_3$  supports this argument and indicates that the two are tightly coupled.

To further test these ideas, we can also look at the trends in the optical signals. We assume the burning time to be the FWHM of the optical signal. This is plotted for the three systems in Fig. 6. The only system that shows a decrease in the burning time as the temperature increases (see Fig. 4 for temperature) is the  $\text{Fe}_2\text{O}_3$  system. For the other two systems, this is not the case. Instead, we see that the burning time does not change over a very wide range of added  $\text{WO}_3$  (0–80%), even when  $\text{WO}_3$  becomes the major component and the temperature increases. Also noteworthy is that the burning time is nearly identical for  $\text{CuO}$  and  $\text{SnO}_2$ , 185 and 210  $\mu\text{s}$ , respectively. This supports our speculation that the burning rate is limited by the aluminum in these two systems, because the aluminum is the only common factor between the two systems. If we compare these burning times to those reported by Bazyn et al. [28] for the combustion of nanoaluminum in a shock tube, we see that our values compare reasonably well. This similarity suggests that the burning of a MIC may resemble the combustion of aluminum in a pressurized oxygenated environment if the oxidizer can decompose efficiently relative to the time scale of the aluminum burning. This behavior was observed for  $\text{CuO}$  and  $\text{SnO}_2$  over almost the entire range of  $\text{WO}_3$ , and it was also seen for the  $\text{Fe}_2\text{O}_3$  when enough  $\text{WO}_3$  was added (80–90%).

Let us discuss this point in the context of a burn tube. As mentioned previously, the pressurization rate has been shown to correlate with the flame propagation velocity. However, this correlation is not quantitative. For example,  $\text{Al/CuO}$  has a pressurization rate on the order of 10  $\text{psi}/\mu\text{s}$  with a flame velocity of 550  $\text{m/s}$ , whereas  $\text{Al/Fe}_2\text{O}_3$  has a pressurization rate of 0.02  $\text{psi}/\mu\text{s}$  with a flame velocity of 25  $\text{m/s}$  (velocities are from unpublished data of burning in an acrylic burn tube and measuring the two-point velocity with photodiodes). We can also look at the difference in burning times measured in this work: 170 and 936  $\mu\text{s}$  for  $\text{Al/CuO}$  and  $\text{Al/Fe}_2\text{O}_3$ , respectively. The pressurization rates are different by a factor of 500, the burning times a factor of 5, and the flame velocities a factor of 20. It is evident that neither the pressurization rate nor the burning time alone can quantitatively predict the flame propagation velocity. We believe the reason for this lies in the discussion of what the rate-limiting step is.

As was discussed previously, one major difference between  $\text{Al/CuO}$  and  $\text{Al/Fe}_2\text{O}_3$  is when the system pressure peaks relative to the optical emission. For  $\text{Al/Fe}_2\text{O}_3$ , both occur at the same time, and so it is reasonable to assume that there should be some direct relationship between the pressurization rate and burn velocity. For  $\text{Al/CuO}$ , however, predicting the propagation velocity is more complicated. In this case, the system is speculated to pressurize quickly via the release of  $\text{O}_2$  gas, followed by the burning of aluminum over a longer time scale. If this is happening, then one would not expect the pressurization rate alone to predict the propagation velocity. Instead, the velocity would be more limited by the aluminum burning. As mentioned in the introduction, convection is considered to be primarily responsible for energy transport through the material. If  $\text{O}_2$  gas is being released quickly, then it would contribute largely to the convection. If we consider a self-propagating flame to be a series of

ignition sites, then upon ignition, the first layer would begin to burn and transfer energy forward. The subsequent unreacted layer will only need to be heated to the ignition point before the flame can continue propagating. To complicate this further, nanoparticles have small characteristic flow relaxation times, meaning that they can be easily swept up and carried forward by the gas. This itself may be an important phenomenon to include in modeling such a system. If a pressure rise is happening fast relative to the burning, it is possible that the  $\text{O}_2$  can pick up unreacted particles and carry them forward, leading to a faster flame velocity than would be predicted by simply looking at the aluminum burning time.

## V. Conclusions

The reaction mechanism of aluminum-based MICs was investigated by simultaneously collecting the pressure and optical signals from combustion in a constant-volume pressure cell. Three oxidizers were studied ( $\text{CuO}$ ,  $\text{SnO}_2$ , and  $\text{Fe}_2\text{O}_3$ ) and were chosen based on their ability to decompose and release  $\text{O}_2$  (and  $\text{SnO}$  for the  $\text{SnO}_2$ ).  $\text{WO}_3$  was blended with the three oxidizers as a means to perturb the system gas release while keeping the system temperature relatively constant when added as the minor component. The results suggest that  $\text{CuO}$  and  $\text{SnO}_2$  decompose to release gaseous oxidizers, leading to a rapid pressurization followed by a longer burn time that is rate limited by the aluminum. For the  $\text{Fe}_2\text{O}_3$ , the experimental data show that the optical and pressure signals occur concurrently. The reaction mechanism in this case is speculated to be rate limited by the oxidizer decomposition. The results suggest that, if oxidizer decomposition is fast relative to the reaction time scale, then the burning of an aluminum-based MIC may resemble the burning of aluminum in a pressurized oxygenated environment.

## Acknowledgment

This work was supported by the U.S. Army Research Office.

## References

- [1] Aumann, C. E., Skofronick, G. L., and Martin, J. A., "Oxidation Behavior of Aluminum Nanopowders," *Journal of Vacuum Science and Technology B (Microelectronics and Nanometer Structures)*, Vol. 13, No. 3, 1995, pp. 1178–1183. doi:10.1116/1.588232
- [2] Umbrajkar, S. M., Schoenitz, M., and Dreizin, E. L., "Exothermic Reactions in Al–CuO Nanocomposites," *Thermochimica Acta*, Vol. 451, Nos. 1–2, 2006, pp. 34–43. doi:10.1016/j.tca.2006.09.002
- [3] Schoenitz, M., Umbrajkar, S., and Dreizin, E. L., "Kinetic Analysis of Thermite Reactions in Al–MoO<sub>3</sub> Nanocomposites," *Journal of Propulsion and Power*, Vol. 23, No. 4, 2007, pp. 683–687. doi:10.2514/1.24853
- [4] Bazyn, T., Glumac, N., Krier, H., Ward, T. S., Schoenitz, M., and Dreizin, E. L., "Reflected Shock Ignition and Combustion of Aluminum and Nanocomposite Thermite Powders," *Combustion Science and Technology*, Vol. 179, No. 3, 2007, pp. 457–476. doi:10.1080/00102200600637261
- [5] Prentice, D., Pantoya, M. L., and Clapsaddle, B. J., "Effect of Nanocomposite Synthesis on the Combustion Performance of a Ternary Thermite," *Journal of Physical Chemistry B*, Vol. 109, No. 43, 2005, pp. 20180–20185. doi:10.1021/jp0534481
- [6] Schoenitz, M., Ward, T. S., and Dreizin, E. L., "Fully Dense Nanocomposite Energetic Powders Prepared by Arrested Reactive Milling," *Proceedings of the Combustion Institute*, Vol. 30, No. 2, 2005, pp. 2071–2078. doi:10.1016/j.proci.2004.08.134
- [7] Moore, D. S., Son, S. F., and Asay, B. W., "Time-Resolved Spectral Emission of Deflagrating Nano-Al And Nano-MoO<sub>3</sub> Metastable Interstitial Composites," *Propellants, Explosives, Pyrotechnics*, Vol. 29, No. 2, 2004, pp. 106–111. doi:10.1002/prep.200400038
- [8] Plantier, K. B., Pantoya, M. L., and Gash, A. E., "Combustion Wave Speeds of Nanocomposite Al/Fe<sub>2</sub>O<sub>3</sub>: The Effects of Fe<sub>2</sub>O<sub>3</sub> Particle Synthesis Technique," *Combustion and Flame*, Vol. 140, No. 4, 2005, pp. 299–309.

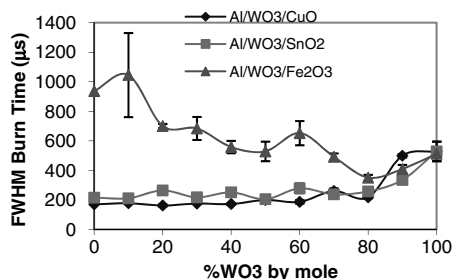


Fig. 6 Experimental FWHM burn time for the three systems as a function of the percentage of  $\text{WO}_3$ .

- doi:10.1016/j.combustflame.2004.10.009
- [9] Clapsaddle, B. J., Zhao, L., Gash, A. E., Satcher, J. H., Jr., Shea, K. J., Pantoya, M. L., and Simpson, R. L., "Synthesis and Characterization of Mixed Metal Oxide Nanocomposite Energetic Materials," *Materials Research Society Symposium Proceedings*, Vol. 800, Synthesis, Characterization and Properties of Energetic/Reactive Nanomaterials, Materials Research Society, Warrendale, PA, 2003, pp. 91–96.
- [10] Kwon, Y.-S., Gromov, A. A., Ilyin, A. P., Popenko, E. M., and Rim, G.-H., "The Mechanism of Combustion of Superfine Aluminum Powders," *Combustion and Flame*, Vol. 133, No. 4, 2003, pp. 385–391. doi:10.1016/S0010-2180(03)00024-5
- [11] Perry, W. L., Smith, B. L., Bulian, C. J., Busse, J. R., Macomber, C. S., Dye, R. C., and Son, S. F., "Nano-Scale Tungsten Oxides for Metastable Intermolecular Composites," *Propellants, Explosives, Pyrotechnics*, Vol. 29, No. 2, 2004, pp. 99–105. doi:10.1002/prep.200400037
- [12] Sanders, V. E., Asay, B. W., Foley, T. J., Tappan, B. C., Pacheco, A. N., and Son, S. F., "Reaction Propagation of Four Nanoscale Energetic Composites (Al/MoO<sub>3</sub>, Al/WO<sub>3</sub>, Al/CuO, and Bi<sub>2</sub>O<sub>3</sub>)," *Journal of Propulsion and Power*, Vol. 23, No. 4, 2007, pp. 707–714. doi:10.2514/1.26089
- [13] Bockmon, B. S., Pantoya, M. L., Son, S. F., Asay, B. W., and Mang, J. T., "Combustion Velocities and Propagation Mechanisms of Metastable Interstitial Composites," *Journal of Applied Physics*, Vol. 98, No. 6, 2005, Paper 064903. doi:10.1063/1.2058175
- [14] Malchi, J. Y., Foley, T. J., Son, S. F., and Yetter, R. A., "The Effect of Added Al<sub>2</sub>O<sub>3</sub> on the Propagation Behavior of an Al/CuO Nano-Scale Thermite," *Combustion Science and Technology*, Vol. 180, No. 7, 2008, pp. 1278–1294. doi:10.1080/00102200802049471
- [15] Puszynski, J. A., Bulian, C. J., and Swiatkiewicz, J. J., "The Effect of Nanopowder Attributes on Reaction Mechanism and Ignition Sensitivity of Nanothermites," *Materials Research Society Symposium Proceedings*, Vol. 896, Multifunctional Energetic Materials, Materials Research Society, Warrendale, PA, 2006, pp. 147–158.
- [16] Puszynski, J. A., Bulian, C. J., and Swiatkiewicz, J. J., "Processing and Ignition Characteristics of Aluminum–Bismuth Trioxide Nanothermite System," *Journal of Propulsion and Power*, Vol. 23, No. 4, 2007, pp. 698–706. doi:10.2514/1.24915
- [17] Prakash, A., McCormick, A. V., and Zachariah, M. R., "Synthesis and Reactivity of a Super-Reactive Metastable Intermolecular Composite Formulation of Al/KMnO<sub>4</sub>," *Advanced Materials*, Vol. 17, No. 7, 2005, pp. 900–903. doi:10.1002/adma.200400853
- [18] Moore, K., Pantoya, M. L., and Son, S. F., "Combustion Behaviors Resulting from Bimodal Aluminum Size Distributions in Thermites," *Journal of Propulsion and Power*, Vol. 23, No. 1, 2007, pp. 181–185. doi:10.2514/1.20754
- [19] Perry, W. L., Tappan, B. C., Reardon, B. L., Sanders, V. E., and Son, S. F., "Energy Release Characteristics of the Nanoscale Aluminum–Tungsten Oxide Hydrate Metastable Intermolecular Composite," *Journal of Applied Physics*, Vol. 101, No. 6, 2007, Paper064313. doi:10.1063/1.2435797
- [20] Son, S. F., Busse, J. R., Asay, B. W., Peterson, P. D., Mang, J. T., Bockmon, B., and Pantoya, M. L., "Propagation Studies of Metastable Intermolecular Composites (MIC)," *Proceedings of the 29th International Pyrotechnics Seminar* Vol. 29, International Pyrotechnics Society, Marshall, TX, 2002, pp. 203–212.
- [21] Rai, A., Park, K., Zhou, L., and Zachariah, M. R., "Understanding the Mechanism of Aluminum Nanoparticle Oxidation," *Combustion Theory and Modelling*, Vol. 10, No. 5, 2006, pp. 843–859. doi:10.1080/13647830600800686
- [22] Trunov, M. A., Schoenitz, M., and Dreizin, E. L., "Effect of Polymorphic Phase Transformations in Alumina Layer on Ignition of Aluminum Particles," *Combustion Theory and Modelling*, Vol. 10, No. 4, 2006, pp. 603–623. doi:10.1080/13647830600578506.
- [23] Trunov, M. A., Schoenitz, M., Zhu, X., and Dreizin, E. L., "Effect of Polymorphic Phase Transformations in Al<sub>2</sub>O<sub>3</sub> Film on Oxidation Kinetics of Aluminum Powders," *Combustion and Flame*, Vol. 140, No. 4, 2005, pp. 310–318. doi:10.1016/j.combustflame.2004.10.010
- [24] Levitas, V. I., Asay, B. W., Son, S. F., and Pantoya, M., "Mechanochemical Mechanism for Fast Reaction of Metastable Intermolecular Composites Based on Dispersion of Liquid Metal," *Journal of Applied Physics*, Vol. 101, No. 8, 2007, Paper 083524. doi:10.1063/1.2720182
- [25] Levitas, V. I., "Burn Time of Aluminum Nanoparticles: Strong Effect of the Heating Rate and Melt-Dispersion Mechanism," *Combustion and Flame*, Vol. 156, No. 2, 2009, pp. 543–546. doi:10.1016/j.combustflame.2008.11.006
- [26] Levitas, V. I., Pantoya, M. L., and Dikici, B., "Melt Dispersion Versus Diffusive Oxidation Mechanism for Aluminum Nanoparticles: Critical Experiments and Controlling Parameters," *Applied Physics Letters*, Vol. 92, No. 1, 2008, Paper 011921. doi:10.1063/1.2824392
- [27] Bazyn, T., Krier, H., and Glumac, N., "Shock Tube Measurements of Combustion of Nano-Aluminum," 44th AIAA Aerospace Sciences Meeting and Exhibit, AIAA Paper 2006-1157, 2006, pp. 1–8.
- [28] Bazyn, T., Krier, H., and Glumac, N., "Combustion of Nanoaluminum at Elevated Pressure and Temperature Behind Reflected Shock Waves," *Combustion and Flame*, Vol. 145, No. 4, 2006, pp. 703–713. doi:10.1016/j.combustflame.2005.12.017
- [29] Bazyn, T., Krier, H., and Glumac, N., "Evidence for the Transition from the Diffusion-Limit in Aluminum Particle Combustion," *Proceedings of the Combustion Institute*, Vol. 31, No. 2, 2007, pp. 2021–2028. doi:10.1016/j.proci.2006.07.161
- [30] Son, S. F., Asay, B. W., Foley, T. J., Yetter, R. A., Wu, M. H., and Risha, G. A., "Combustion of Nanoscale Al/MoO<sub>3</sub> Thermite in Microchannels," *Journal of Propulsion and Power*, Vol. 23, No. 4, 2007, pp. 715–721. doi:10.2514/1.26090
- [31] Hobbs, M. L., Baer, M. R., and McGee, B. C., "JCZS: An Intermolecular Potential Database for Performing Accurate Detonation and Expansion Calculations," *Propellants, Explosives, Pyrotechnics*, Vol. 24, No. 5, 1999, pp. 269–279. doi:10.1002/(SICI)1521-4087(199910)24:5<269::AID-PREP269>3.0.CO;2-4

S. Son  
Associate Editor